ScienceAdvances

www.advances.sciencemag.org/cgi/content/full/1/6/e1500093/DC1

Supplementary Materials for

High geothermal heat flux measured below the West Antarctic Ice Sheet

Andrew T. Fisher, Kenneth D. Mankoff, Slawek M. Tulaczyk, Scott W. Tyler, Neil Foley, and the WISSARD Science Team

WISSARD Science Team Members: W. P. Adkins, S. Anandakrishnan, G. Barcheck, L. Beem, A. Behar, M. Beitch, R. Bolsey, C. Branecky, R. Edwards, A. T. Fisher, H. A. Fricker, N. Foley, B. Guthrie, T. Hodson, H. Horgan, R. Jacobel, S. Kelley, K. D. Mankoff, E. McBryan, R. Powell, A. Purcell, D. Sampson, R. Scherer, J. Sherve, M. Siegfried, S. Tulaczyk

Published 10 July 2015, *Sci. Adv.* **1**, e1500093 (2015)
DOI: 10.1126/sciadv.1500093

This PDF file includes:

Supplementary Materials

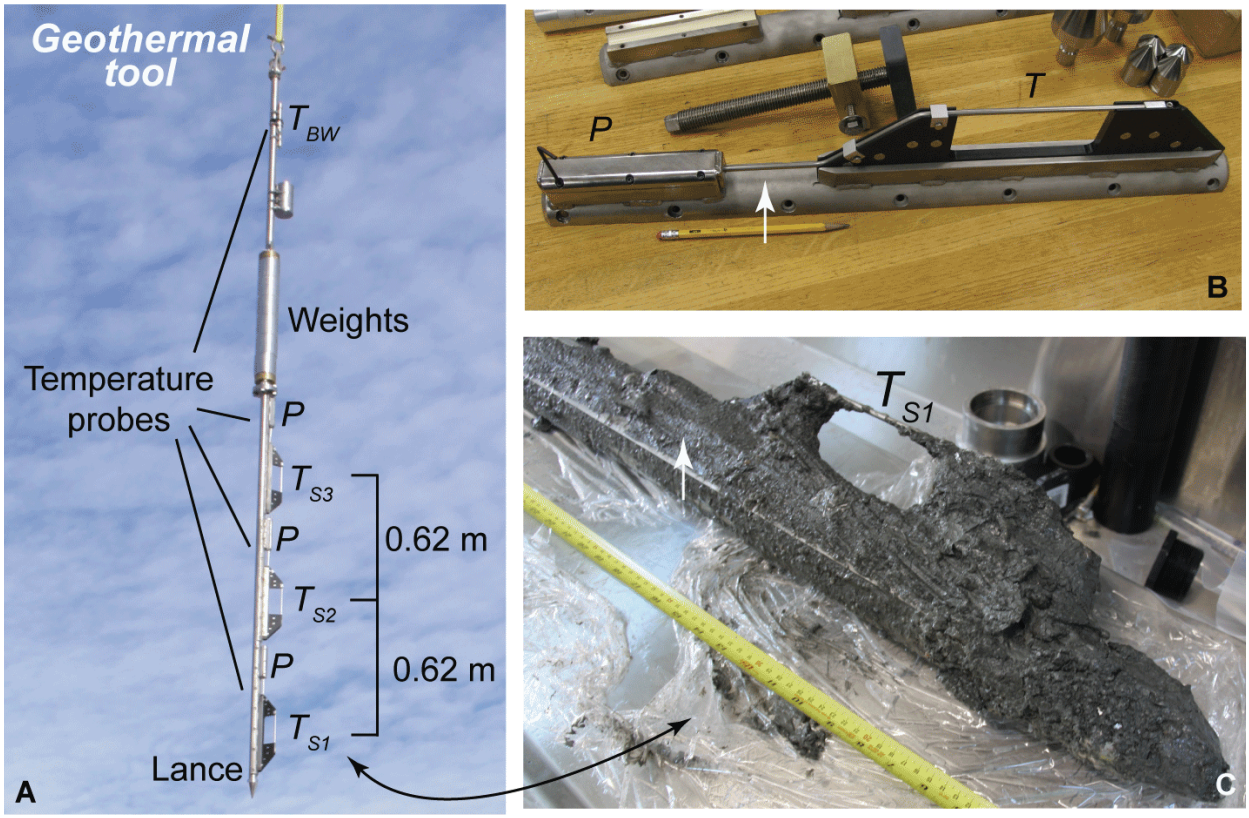

Figure S1
Fisher et al.

Figure S1. WISSARD GT deployed below SLW. **A.** Geothermal tool as prepared immediately prior to the first deployment below SLW. Sediment temperature probes are mounted on the lance with pressure cases (*P*) positioned above the sensors (T_{Sx}, x = 1, 2, 3), and bottom water sensor (T_{BW}) is mounted above the weights. Autonomous temperature probe mounted on outrigger assembly prior to attachment to lance. *T* = thermistor sensor, *P* = pressure case below "clam-shell" cover. White arrow shows area where sensor tube stands off from outrigger mount by about 1 cm. **C.** Lower outrigger mount and temperature probe (sensor T_{S1}) following instrument recovery after first deployment below SLW. The sticky sediment caked on the tool helped to determine depth of penetration. White arrow shows region where mud is tightly packed into area between sensor tube and outrigger mount (occurred on both deployments). An equivalent location above the second sediment sensor was free of mud after both deployments, as were other locations where mud would tend to stick and be protected by the sensor mount, setting an upper limit on the depth of burial.

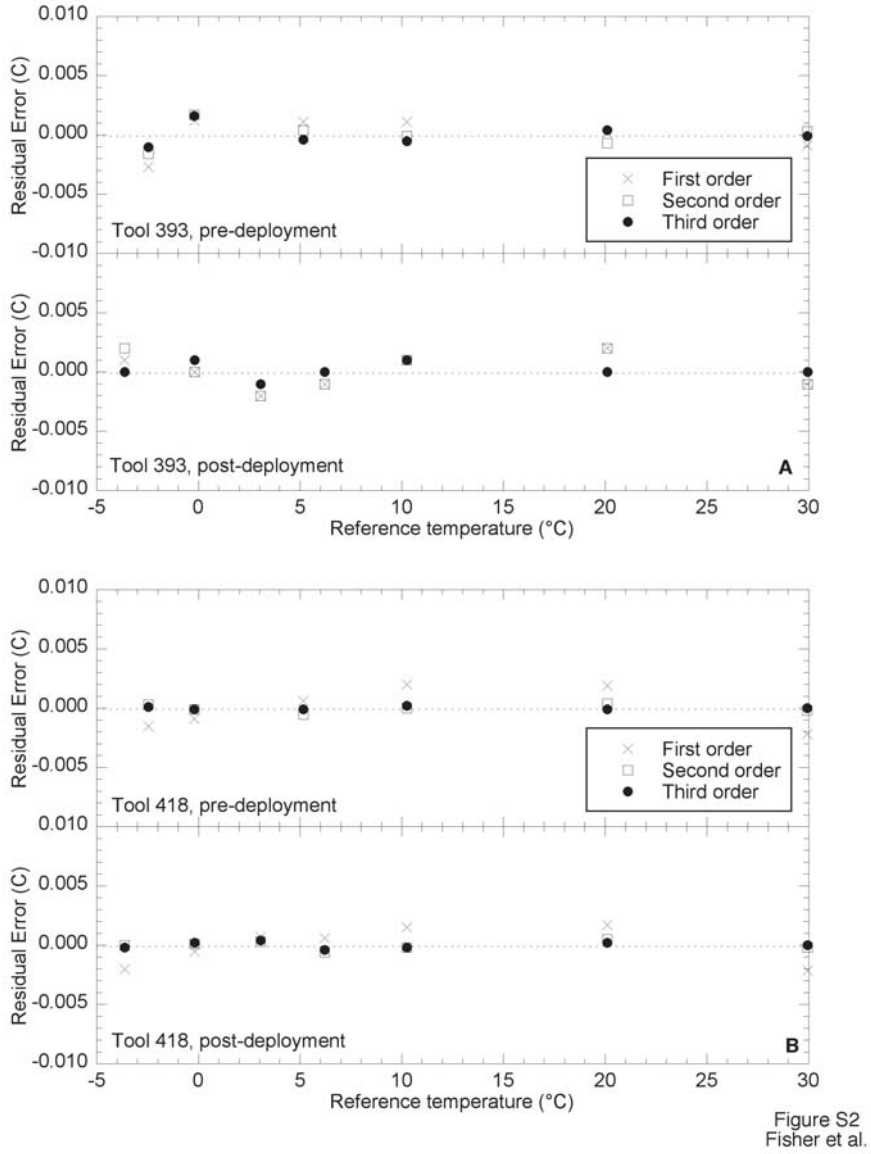

Figure S2. Example calibration results from two autonomous probes used with the WISSARD GT deployed below SLW. For each of two probes, pre- and post-deployment caliubration is shown, with a listing of residual temperature errors following application of first, second, and third order polynomial fits to match probe data to results from a NIST-traceable RTD sensor. **A.** Calibration results for the probe used for bottom water temperature (T_{BW}, Tool 393. **B.** Calibration results for one of the probes used for sediment temperature (T_{S1}, Tool 418).

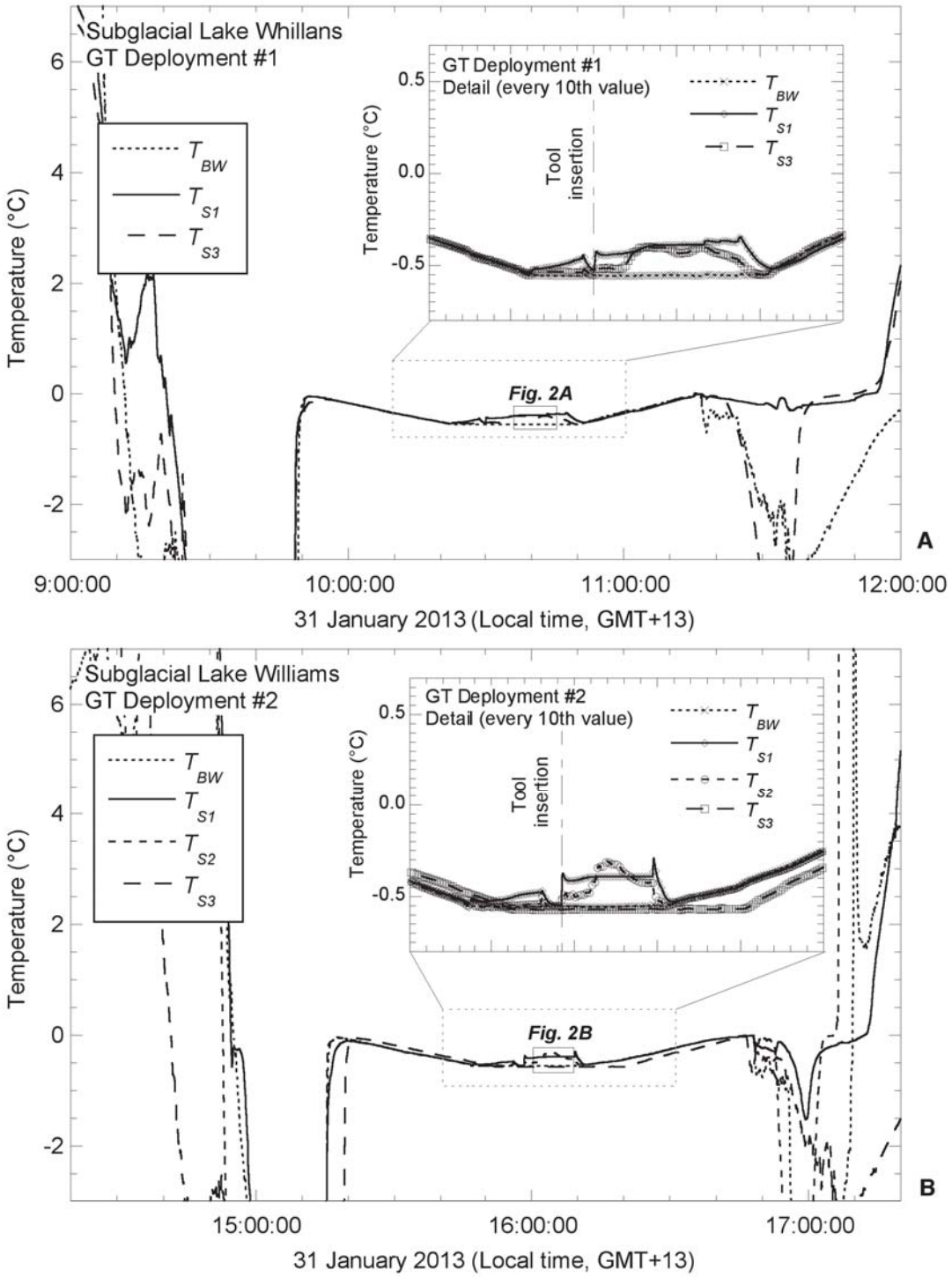

Figure S3. Complete records from GT deployments below SLW. Data were collected every 2 seconds. **A.** Complete record from GT deployment 1, with inset showing 50-minute detail (symbol for every 10th value). Data are not shown for Tool T_{S2}, which suffered an electronic fault. Data shown in **Fig. 2A** in main paper are indicated by small box. **B.** Complete record from GT deployment 2, with inset showing 50-minute detail (symbol for every 10th value). Data shown in **Fig. 2B** in main paper are indicated by small box.

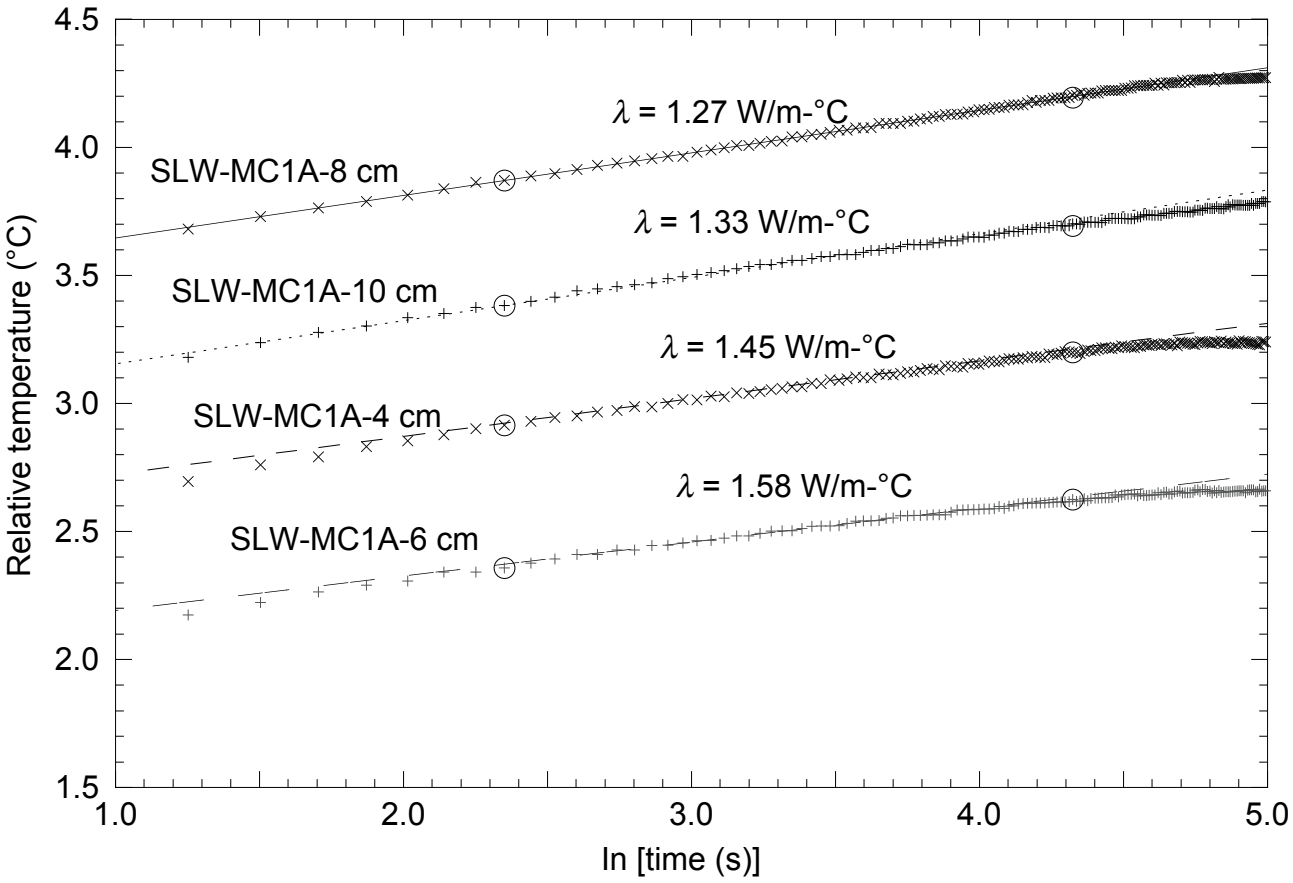

Figure S4. Example records from needle-probe thermal conductivity determinations made on a core sample recovered from the bottom of SLW. Four records are shown, and temperatures have been offset by 0.5°C for display, with data collected every 0.5 second. Every second value is shown for clarity. The large circles show the start and end of the data interval used to determine the thermal conductivity, as described in Materials and Methods in the main text.

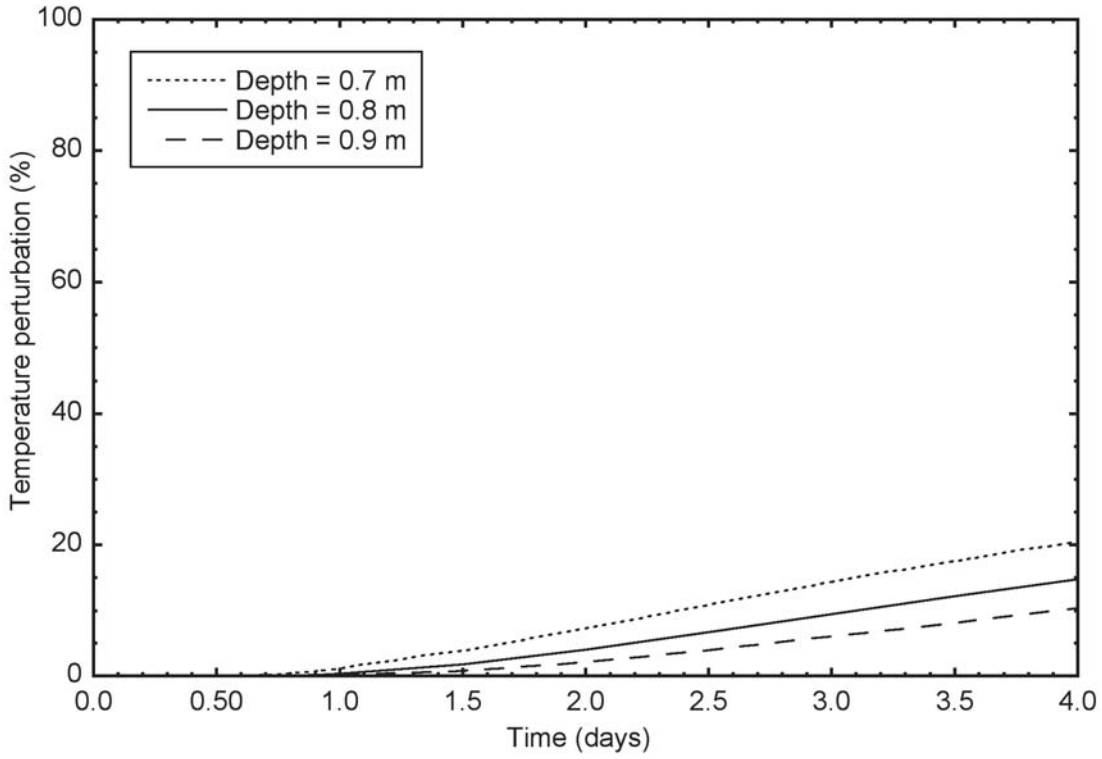

Figure S5

Figure S5. Calculations of the thermal disturbance that could occur as a function of time owing to an abrupt change in bottom water temperature or an adjacent tool insertion. The depth of penetration of the GT was ~0.8 m during both deployments.

Table S-1. Physical parameters used to fit the 2014 DTS data to a one-dimensional, steady-state conduction-advection model

Parameter	Value
T_T	–23.1 °C
T_B	–0.56 °C
z_T	802 m
κ	1.09×10^{-6} m^2/s